The rates of dissolution of olivine, plagioclase, and quartz in a basalt melt

COLIN H. DONALDSON

Department of Geology, University of St Andrews, St Andrews, Fife, KY16 9ST, Scotland

ABSTRACT. The dissolution rates of spheres of two magnesian olivines, two plagioclases, and quartz in tholeiitic basalt have been determined at three super-liquidus temperatures and one-atmosphere pressure. There are considerable differences in the rates among the minerals, e.g. at 1210°, 12° above the liquidus temperature of the basalt, labradorite dissolves at 86 μm/h. and the magnesian olivines at 9 and 14 μm/h. The rates are not time dependent and this, coupled with the existence of concentration gradients in the composition of quenched melt adjacent to partially dissolved crystals, indicates that the dissolution rates are dictated by a combination of diffusion and convection of components to and from the crystal–liquid interface. Values for the activation enthalpy of dissolution are small for quartz and plagioclase (40–50 kcal mol^{-1}) but large for olivine 73–118 kcal mol^{-1}). Dissolution of plagioclase in rock melts seems to be a much more rapid process than crystal growth, whereas olivines apparently dissolve and grow at similar rates. Crystal dissolution is sufficiently slow that ascending, crystal-bearing magma may become superheated and yet fail to dissolve the crystal fraction before quenching; this may be the reason that olivine phenocrysts are often rounded.

KEYWORDS: olivine, plagioclase, quartz, tholeiite, basalt, dissolution.

WHEREAS the kinetics of magmatic crystallization have been of great interest in the last decade (see Dowty, 1980 and Kirkpatrick, 1980, for recent reviews), comparatively little work has been done on the dissolution of minerals in silicate melts of rock or rock-like compositions (Table I). Yet there is an ever-growing body of literature containing evidence of the interaction of mafic magmas with crustal materials (e.g. see papers in Moorbath et al., 1984) and a number of situations are likely in which dissolution may occur. For example, when country rock is accidentally incorporated in a magma, when a primary magma carrying restite crystals ascends speedily from its source, or when a water-undersaturated magma containing phenocrysts moves upwards, and when porphyritic magma, resident in a chamber, is heated by, and/or mixes with a new batch of more primitive magma entering the chamber. Knowledge of dissolution kinetics of minerals in rock melts and an understanding of what controls these kinetics can provide a better sense of what happens during these interactions between crystals and liquid.

This paper presents data on the dissolution rates

Table I. Summary of previous studies of mineral dissolution in silicate melt

Reference	Melt composition	Crystal dissolved	Pressure
Kutolin and Agafanov, 1978	Alkalic basalt	Olivine, garnet, orthopyroxene, clinopyroxene	1 bar
Donaldson, 1979a	Alkali olivine basalt	Olivine	1 bar
Scarfe et al., 1980	Alkali olivine basalt	Olivine, orthopyroxene, clinopyroxene, spinel, garnet	12.5–20 kbar
Watson, 1982	Tholeiitic basalt	Quartz, oligoclase, K-feldspar	1 bar
Thornber and Huebner, 1982	Synthetic lunar basalt	Olivine	1 bar
Kuo and Kirkpatrick, 1983	Melts in the system $CaMgSi_2O_6$–Mg_2SiO_4–SiO_2	Forsterite, diopside, enstatite, quartz	1 bar
Harrison and Watson, 1983	Obsidian	Zircon	8 kbar

of several common rock-forming minerals in a common magma (tholeiitic basalt), at several temperatures. The data, and electron probe microanalyses of the quenched melt near crystal–liquid junctions, are used to examine the factors that limit the rate of mineral dissolution in magmas. Dissolution is shown to be rapid by comparison with crystal growth rates and dissolution rates differ considerably from mineral to mineral.

Experimental

Method. The experiments were conducted at atmospheric pressure in a 3 cm ID vertical muffle tube, set in a Deltech VT-31D furnace. Temperature at the 'hot-spot' of the furnace, was measured with a $Pt_{100}-Pt_{87}Rh_{13}$ thermocouple and a digital thermometer which has 1 °C resolution and $\pm 1°$ accuracy. The thermocouple was calibrated against the melting point of gold.

Oxygen partial pressure was controlled by downwards flow of a CO and CO_2 mixture at 60 cm^3/ min. The p_{O_2} at the 'hot spot' was measured with a ZrO_2–CaO electrolytic cell, calibrated by bracketing the Fe–FeO reaction. It was controlled within 0.3 log units of the quartz–fayalite magnetite buffer, i.e. close to values typical of terrestrial basalts (Sato, 1978). (One consequence of using hydrogen-free gases to control p_{O_2} is that the basalt melt will be nominally anhydrous. Users of the data reported here should note this point as the larger viscosity than is likely in nature will result in slower rates of dissolution than in nature.)

A charge was suspended from a ceramic rod and quenched into either air or water (cooling rates of 200 and $500°/\mathrm{sec}^{-1}$, respectively).

The sample was held on a 3 mm-diameter loop of 0.125 mm diameter platinum wire (Donaldson *et al.*, 1975). A pressed, 35–40 mg pellet of powdered basalt rock (or rarely glass), surrounding a small crystal sphere, was tacked to the wire by passing a small electric current through the wire until the parts of the pellet touching it fuse (Donaldson *et al.*, 1975).

Once at the furnace hot-spot, the basalt fraction fuses as a drop on the wire loop. The maximum size of mineral grains in the pulverised basalt is 5 μm and Donaldson (1979*a*) has shown that complete fusion, 5° above the liquidus temperature, occurs within a few minutes. In the present experiments at > 12 °C above the liquidus fusion of the basalt will be nearly instantaneous.

In a few experiments reported here powdered rock and a crystal sphere were reacted in the melting interval of the rock, as much as 70° below the liquidus temperature. Melt appeared virtually instantly, however, the full amount of melt and its

Table II. Composition of basalt used in experiments

SiO_2	51.91
TiO_2	1.16
Al_2O_3	15.85
Cr_2O_3	0.06
Fe_2O_3	1.65
FeO	8.27
MnO	0.15
MgO	7.01
CaO	8.66
Na_2O	3.03
K_2O	0.75
P_2O_5	0.17
H_2O total	0.86
	99.53

equilibrium composition were not achieved for roughly 1 to 3 hours.

Rock and minerals used. The basalt used is a tholeiite (Table II) with 0.4 wt. % of normative quartz; it is saturated with olivine (Fo_{83-84}) at its liquidus temperature of $1198 \pm 2°$ followed by plagioclase (An_{64}) at 1187°, clinopyroxene at 1133° and magnetite and ilmenite near the solidus at 1090° (Lofgren, 1983). At the three isotherms investigated (1300°, 1250°, and 1210°) the viscosity of the basalt melt is 220, 370, and 560 poise, as computed by the method of Shaw (1972). At the p_{O_2} used losses of Fe to the wire and volatilization of Na and K are minor (Donaldson, 1979*b*) and will not affect the results.

Crystals (Table III) came from the St Andrews mineral collection.*

During dissolution the melt fraction of a charge changes slightly; a typical 1 mm diameter quartz crystal represents approximately 4 % of the mass of a charge and the amount of SiO_2 in the melt would rise by *c*.2 wt. %, if the crystal completely dissolved in the basalt. The same is not true of the melt at the interface between a dissolving quartz crystal and the basaltic melt.

The final column of Table III indicates the fusion characteristics of the various crystals used, in the absence of the basalt solvent. At the temperatures at which the experiments were conducted (1120–1300°), the olivines and quartz do not melt and the labradorite would melt only slightly at 1300°; on the other hand, the oligoclase could partially melt

---

* Pyroxene is conspicuous by its absence from Table III. In the melt used both orthopyroxene and augite undergo a complex dissolution reaction in which pyroxene destruction is accompanied by the crystallization of very small crystals of olivine around the pyroxene. The process will be described in another article.

Table III. Crystals used and their origin

Mineral	Comments	Origin	Fusion characteristics in absence of basalt
Olivine, Ig.	$Fo_{91.6}$ (ave. of 12 'probe analyses; spread of values <2% Fo); glassy green; inclusion-free	Phenocrysts from the Iglorrsuit picrite sill Ubekendt Ejland, West Greenland	Solidus ca. $1760°$, liquidus ca. $1850°$ (Bowen and Schairer, 1935)
Olivine, H19	$Fo_{88.6}$ (ave. of 6 'probe analyses; spread of values < 2% Fo); glassy yellow; scarce inclusions of chrome spinel	Phenocrysts in picritic basalt lava, Mauna Loa, Hawaii	Solidus ca. $1740°$, liquidus ca. $1840°$ (Bowen and Schairer, 1935)
Labradorite	$An_{52.5} Or_{2.9} Ab_{44.6}$ (ave. of 10 'probe analyses; spread of An values <3%); cloudy white	Anorthosite, Michikamau intrusion, Labrador	Solidus $1290°$, liquidus $1435°$ At $1300°$ under equilibrium conditions thers should be 2.5% liquid. (Bowen, 1913)
Oligoclase	$An_{29.0} Or_{3.4} Ab_{67.6}$ (ave. of 9 'probe analyses; spread of An values <7%); cloudy white	Pegmatite, Isle of Lewis, Scotland	Solidus $1180°$, liquidus $1380°$ At $1210°$ should be 16.5% liquid, and at $1300°$ 61% liquid. (Bowen, 1913)
Quartz, G	Colourless, transparent, inclusion-free	Vein quartz, San Jose Main Vein, Llallagua, Bolivia	Melts at $1713°$
(Quartz[1], C	Crystals with strained (undulose) extinction	Granodiorite, Criffel intrusion, Scotland)	
(Quartz[1], T	Cloudy white	Phenocrysts from rhyolite, Tibchi complex, Nigeria)	

[1] Very few experiments conducted with these crystals (see Table 4)

in all the experiments above 1180°. In experiments in which plagioclase is dissolved in basalt, except those with oligoclase at 1300°, there is no clear evidence of internal melting of the crystals, nor is there an enveloping film of plagioclase glass separating crystal from basalt. This implies that dissolution rates of plagioclase in basalt exceed the fusion rates of the crystals. The exception, oligoclase at 1300°, melts in approximately twenty minutes and it is this blob of melt that proceeds to dissolve in the basalt.

Mineral sphere preparation and measurement. The spheres used range from 0.5 to 1.5 mm in diameter, with most being 0.6 to 0.9 mm. They were prepared in a mini-tumbler, as described by Bond (1951): roughly equant mineral chips are blown around the inside of a 1.5 cm diameter brass cylinder lined with carborundum-coated paper. By rejecting roughly seventy percent of all the 'spheres' obtained, crystals with a 'high' degree of sphericity can be obtained, in which diameters measured in any direction differ by less than $\pm 5\%$ of the average of ten measurements, in random orientations, using a microscope equipped with an eyepiece graticule.

Post-experiment observations. One means of determining dissolution rates is to conduct a series of isothermal experiments of different duration on crystals of uniform size, and thereby establish the minimum time needed to completely destroy that size of crystal. The rate of dissolution would then be taken as the crystal size divided by the minimum

time established from the experiments. The drawback to this approach is that it would not reveal whether the dissolution rate was time dependent, as it would be if it is controlled purely by diffusion of material in the melt. It is more informative to conduct a series of experiments of different durations at each isotherm and determine the change in size of the crystal spheres: then a graph of run duration versus the change in size will reveal any time dependence.

To determine the change in size of a sphere requires measuring the post-experiment size of the crystal. This is done by gluing the charge to a glass slide and then hand-grinding with carborundum powder. Once the crystal is exposed, its diameter is measured between successive 30-second grindings and the maximum value is taken as the diameter of the sphere. This value is considered accurate to ± 0.02 mm. In many charges, notably of quartz, oligoclase, and olivine, the crystal remnant is close enough to the surface to be measured with a binocular microscope; agreement with the other method is excellent.

If required, the now-flattened surface of the charge can be mounted on a glass slide and a thin section prepared. A small proportion of the charges were prepared as polished thin sections and the electron probe used to examine the composition of the glass near to crystals.

The probe analyses were obtained on the Cambridge Instruments Mark V machine in the Edinburgh University Geology Department. Individual

C. H. DONALDSON

Table IV. Data for individual runs

Run no	Crystal	Temp. °C	Duration, hours	Init. diam. mm	Final diam. mm	Δradius, mm	correlation coefficient	intercept on Δradius axis, mm	dissolution rate, μm/hr
217	Quartz, G	1300	1.50	0.60	0.35	0.125			
218	"	"	3.66	1.02	0.46	0.28			
220	"	"	1.42	0.75	0.55	0.10	0.93	0.005	78
319	"	"	0.50	0.53	0.43	0.05			
320	"	"	3.01	0.85	0.33	0.26			
243	Quartz, G	1250	4.08	0.60	0.24	0.18			
246	"	"	2.0	0.62	0.47	0.075			
261	"	"	2.75	0.60	0.30	0.15			
262	"	"	1.53	0.85	0.73	0.075			
277	"	"	1.00	0.52	0.44	0.04			
280	"	"	1.00	1.00	0.91	0.045	0.98	-0.010	51
290	"	"	1.00	1.02	0.92	0.05			
299	"	"	2.25	0.70	0.46	0.12			
300	"	"	5.17	1.65	1.13	0.26			
261a	"	"	2.75	0.65	0.37	0.14			
261b	"	"	2.75	0.67	0.39	0.14			
299	Quartz, T	"	2.25	0.70	0.46	0.12			
300	"	"	5.05	1.50	1.08	0.26			ave.53
300a	"	"	5.30	1.72	1.14	0.29			
399	Quartz, C	"	4.60	0.85	0.37	0.24			
390	"	"	3.21	0.83	0.67	0.18			ave.56
391	"	"	1.25	0.84	0.69	0.075			
193	Quartz, G	1210	25.25	0.52	0	0.26			
194	"	"	17.0	0.60	0	0.30			
195	"	"	2.5	0.60	0.45	0.07			
196	"	"	9.33	0.52	0	0.31	0.95	-0.011	36
312	"	"	1.01	0.82	0.76	0.03			
320	"	"	5.08	0.85	0.50	0.175			
392	"	"	3.92	0.63	0.33	0.15			
292	"	1143	72.0	1.01	0.76	0.125			
293	"	"	72.0	0.98	0.70	0.14			
338	"	"	24.25	0.52	0.45	0.035	0.57	0.059	0.4
339	"	"	163.0	0.82	0.57	0.123			
340	"	"	149.2	1.22	0.91	0.153			
301	"	1122	145.5	1.70	1.61	0.045			
302	"	"	169.75	0.50	0.21	0.075			ave. 0.38
222	Oligoclase	1300	1.0	0.98	0.53	0.225			
324	"	"	0.45	1.01	0.73	0.14			
325	"	"	0.18	0.72	0.62	0.05	0.98	-0.011	205
326	"	"	0.57	0.85	0.55	0.15			
326a	"	"	0.68	0.79	0.51	0.14			
255	"	1250	1.25	0.50	0.14	0.18			
256	"	"	2.0	0.52	0	0.26			
257	"	"	1.75	1.02	0.52	0.25	0.92	-0.006	147
288	"	"	1.0	1.01	0.71	0.15			
289	"	"	1.0	1.20	0.94	0.13			
186	"	1210	0.75	0.61	0.46	0.075			
190	"	"	5.58	0.60	0	0.3			
192	"	"	3.0	0.62	0.12	0.25	0.90	0.022	77
332	"	"	0.5	0.75	0.63	0.06			
333	"	"	1.83	0.95	0.60	0.175			
294	"	1150	70.0	1.52	0.72	0.40			6
219	Labredorite	1300	1.0	0.62	0.26	0.18			
221	"	"	1.5	1.02	0.38	0.32			
321	"	"	0.75	0.65	0.31	0.17	0.98	-0.014	213
322	"	"	0.5	0.75	0.60	0.075			
323	"	"	0.25	0.75	0.63	0.06			
247	"	1250	1.42	0.55	0.21	0.17			
258	"	"	1.75	0.60	0.21	0.195			
259	"	"	1.90	0.45	0	0.225	0.89	-0.009	114
281	"	"	1.15	0.90	0.68	0.11			
282	"	"	1.78	1.03	0.67	0.18			
330	"	"	0.52	0.70	0.60	0.05			
184	"	1210	1.67	0.50	0.35	0.115			
187	"	"	2.25	0.52	0.37	0.175			
334	"	"	2.0	0.80	0.54	0.13	0.99	-0.014	86
335	"	"	0.57	0.82	0.78	0.02			
336	"	"	1.0	0.65	0.53	0.06			
208	Olivine Ig.	1300	2.08	0.50	0.08	0.21			
209	"	"	1.20	0.50	0.30	0.10	0.92	-0.012	83
209a	"	"	1.20	0.54	0.29	0.125			
210	"	"	3.00	0.60	0	0.30			
133	"	1250	2.0	0.50	0.25	0.125			
134	"	"	1.0	0.51	0.46	0.025			
135	"	"	4.0	0.50	0.20	0.15			
136	"	"	5.0	0.51	0.23	0.14			
137	"	"	3.0	0.65	0.50	0.075	0.85	0.015	24
266	"	"	2.75	0.50	0.35	0.075			
267	"	"	4.08	0.70	0.55	0.075			
274	"	"	1.5	0.40	0.30	0.05			
275	"	"	1.5	0.45	0.35	0.05			
276	"	"	3.0	0.40	0.17	0.115			
149	"	1210	2.0	0.40	0.26	0.02			
150	"	"	5.0	0.40	0.25	0.075			
151	"	"	6.67	0.42	0.27	0.075	0.83	0.022	8.7
152	"	"	17.58	0.43	0.23	0.10			
153	"	"	12.0	0.44	0.19	0.125			
211	Olivine, H19	1300	3.08	0.55	0.18	0.19			ave. 63.5
212	"	"	1.50	0.60	0.40	0.10			
139	"	1250	4.0	0.60	0.40	0.10			
140	"	"	1.03	0.50	0.45	0.025			
142	"	"	2.0	0.50	0.42	0.04			
154	"	"	16.67	0.55	0	0.275			
155	"	"	5.5	0.45	0.10	0.175			
155a	"	"	5.5	0.48	0.18	0.15			
156	"	"	10.67	0.40	0	0.2			
160	"	"	8.17	0.45	0	0.225	0.92	-0.003	26
163	"	"	6.92	0.40	0	0.20			
268	"	"	6.42	0.50	0.20	0.15			
272	"	"	1.5	0.45	0.38	0.035			
273	"	"	3.0	0.40	0.24	0.08			
296	"	"	3.0	0.61	0.43	0.09			
297	"	"	1.5	0.50	0.44	0.02			
298	"	"	4.08	0.81	0.59	0.11			
308	"	"	9.5	1.01	0.53	0.24			
306	"	1210	2.5	0.55	0.49	0.03			
307	"	"	6.0	0.56	0.40	0.08			
178	"	"	24.0	0.40	0.20	0.10	0.99	-0.006	14
179	"	"	46.75	0.39	0.17	0.11			
180	"	"	96.0	0.51	0.32	0.095			

wavelength-dispersive analyses were obtained of 2 μm-wide spots along a traverse at right angles to the crystal–glass interface. Full ZAF corrections were applied.

Errors and reproducibility of results. In obtaining a value for the change in diameter of a sphere there are two main sources of error: (i) the imperfect sphericity of the crystals and (ii) the errors in measuring the crystals before and after the experiment. It is estimated that the total error attached to each value of the change in crystal radius (Δr) in Table IV is ± 0.035 mm.

The reproducibility of results was examined in a small number of experiments carried out on quartz crystals at the same temperature (1250°) and two different run times (1.0 and 2.75 hours). The results (Table IV) show reasonable agreement in the values of Δr, the spread in values being 0.01 mm for both run times.

A useful conclusion to be drawn from these estimates is that to obtain results of greater accuracy would require either (*a*) the use of bigger crystals or (*b*) the ability to observe the dissolving crystals directly. Neither approach is free of problems: (*a*) requires longer run times and larger volumes of melt than can be held on wire loops, and the resultant need for a crucible will result in greater iron loss; (*b*) quite simply is impossible because Fe-bearing melts are opaque—only model, Fe-free, melts could be studied.

Results

Dissolution rates. The results of the individual experiments conducted are recorded in Table IV, and an example of a crystal that has been partially dissolved is shown in fig. 1. Fig. 2 shows a typical
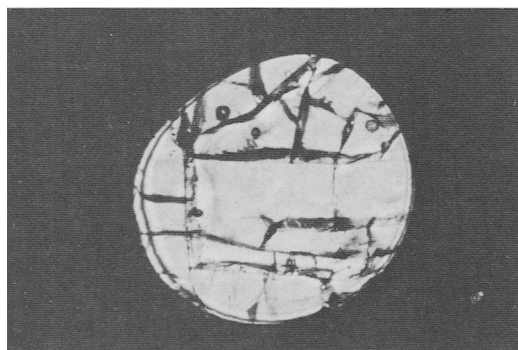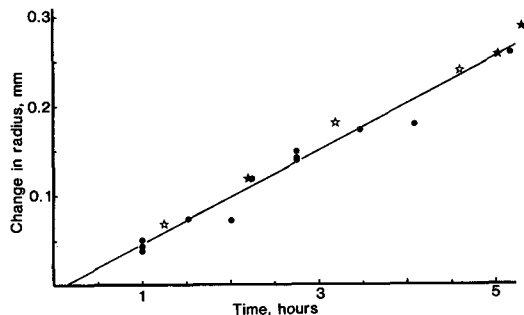
FIG. 2. Plot of time versus change in sphere radius for all runs conducted on quartz at 1250°. Filled circles are quartz G, filled stars are quartz T and unfilled stars are quartz C. The line is obtained by linear regression of the quartz G data

plot of Δr against run duration. The data points conform to a coherent straight line that passes very close to the origin of the graph. Simple linear regression analysis has been used to obtain the equation of the line: the slope of the line (i.e. the dissolution rate), its intercept on the vertical axis of the graph and the correlation coefficient are listed in Table IV. The same information is provided for groups of experiments at the same temperature involving the same mineral, in Table IV. Throughout the Table the correlation coefficient is good and the intercept on the vertical axis is typically small.

The dissolution rates are collated in Table V. All the rates vary exponentially with temperature (fig. 3 and next section). Considerable differences in dissolution rate exist, with the plagioclases dissolving more rapidly than quartz which in turn dissolves more rapidly than the two olivines (except olivine Ig. at 1300°), (cf. Lacroix's (1893) inferences about relative dissolution rates based on petrographic observations of xenocryst-containing basalts). The effect of solid-solution composition on dissolution rate is not clear-cut: the oligoclase and labradorite crystals dissolve at very similar rates (allowing for experimental error), whereas the slightly more magnesian olivine (Ig.) dissolves more rapidly than H19 at 1300° but more slowly than H19 at 1210°.

Comparison of the data obtained for quartz dissolution in this study with that reported by Watson (1982) shows a factor of approximately two difference: this is reasonable, considering that different crystals, different basalts, and different run techniques were employed in the two studies.

Some quartz dissolution experiments (Table IV) were conducted at 1250° on a strained crystal and some on a crystal obtained as phenocrysts from a lava (Table III). The values of Δr against run

FIG. 1. Photomicrograph of a sphere of olivine that has been partially dissolved for 4 hours at 1250° in basalt. Note that the crystal has remained spherical (run 267; XPL; crystal is 0.55 mm in diameter).

Table **V.** Collation of dissolution rates (μm/hr) in Table **IV.**

T °C	Quartz	Oligoclase	Labradorite	Olivine Ig.	Olivine H19
1300	78	205	213	83	63.5
1250	51	147	114	24	26
1210	36	77	86	8.7	14
1150	-	6	-	-	-
1143	0.4	-	-	-	-
1122	0.38	-	-	-	-

duration (open star and filled star symbols, respectively, in fig. 2) reveal no significant differences in dissolution rates among the crystals from the three quite different environments (hydrothermal, plutonic (and strained) and volcanic). Apparently any differences between these crystals with respect to minor- and trace-element contents and defects (*sensu lato*) do not influence the rate at which atoms are removed from the surface of the quartz.

In fig. 3 the three high-temperature data points are for quartz dissolution in basalt melt that is absolutely superheated (i.e. above the liquidus temperature) and the other two involve dissolution in partially melted basalt. Note that the two low-temperature points fall considerably below the extension of the curve extrapolated from the three high-temperature points. There are several possible reasons for this: 1, the melt fraction of the partially melted basalt is likely to be more siliceous than the completely molten basalt, and hence more viscous than supercooled basalt melt at the same temperature. Transport of dissolved quartz components away from the crystal therefore will be inhibited. 2, at these lower temperatures plagioclase is a stable phase and hence the melt is likely to be far more polymerized than supercooled, plagioclase-free basalt melt at the same temperature; this too would result in a relatively large viscosity and sluggish transport of quartz components away from the crystal-liquid interface. 3, at both the lower temperatures there develops about the quartz crystals a continuous fringe of elongate pigeonite crystals, as dissolution proceeds (fig. 4; cf. Sato, 1974); this fringe will tend to extend the distance through which quartz components have to migrate in moving away from the quartz-melt interface and hence reduce dissolution rate; it will also inhibit any convection of melt that might occur near to the crystal (see later section), i.e. reduce the rate of transport of quartz components in the melt.

'*Activation enthalpies*' *of dissolution and their implications*. Since the dissolution rates increase exponentially with temperature the Arrhenius relationship is expected to apply:

$$Z = A_o e^{-(\Delta H/RT)}$$

where Z is dissolution rate at absolute temperature, T, ΔH is the apparent enthalpy of activation of the dissolution reaction, A_o is a constant, the 'frequency
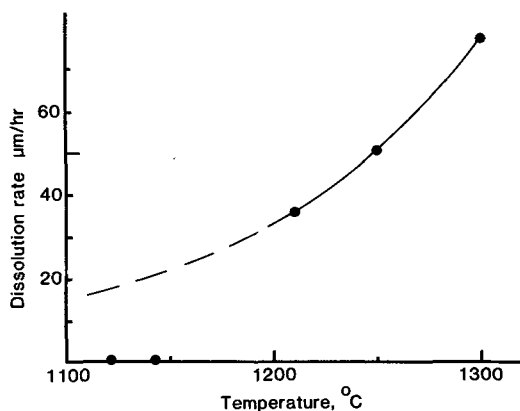
FIG. 3. Plot of temperature versus dissolution rate of quartz G. Note how the measurements at 1122° and 1143° fall well below the extrapolation of the higher temperature data.
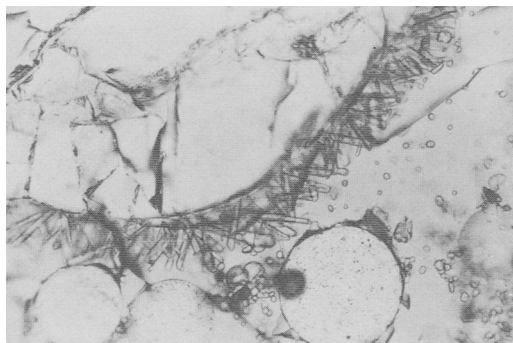
FIG. 4. Photomicrograph of the boundary between a partially dissolved quartz crystal and basalt glass, showing the elongate pigeonite crystals that form a felty texture about the quartz (run 292; PPL; width of view is *c*.0.7 mm).
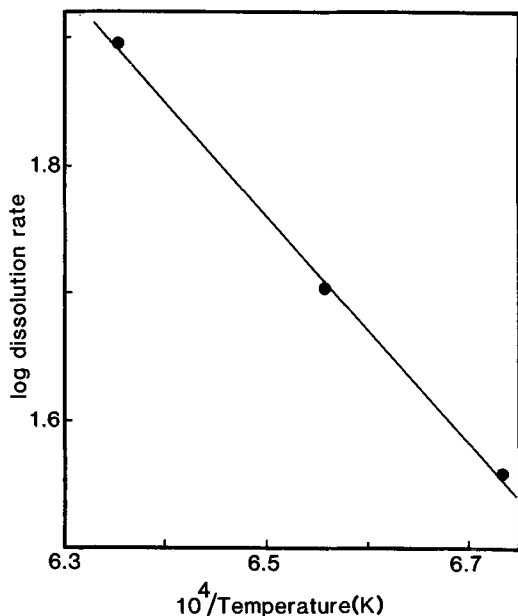
FIG. 5. Arrhenius plot of the dissolution rates of quartz at 1210°, 1250° and 1300°. The line is that obtained by linear regression.

Table VI.

Computed values of activation enthalpy of dissolution, using data in Table **V** and the Arrhenius relationship, and comparison with other studies

Mineral	$-\Delta H$, Kcal mol^{-1}
Quartz	40.3
Oligoclase	50.0
Labradorite	47.7
Olivine Ig.	117
Olivine H19	72.8
Olivine in two lunar basalts (computed from data of Turnock and Huebner, 1982)	268, 213
Quartz in tholeiite (computed from data of Watson, 1982)	~ 45

factor', and R is the gas constant. Plots of $\log Z$ versus $1/T$ were prepared (e.g. fig. 5) and give the value of the slopes $-(\Delta H/R)$ used to obtain $-\Delta H$ (Table VI). For each of the five minerals, the three data points at the temperatures 1210°, 1250° and 1300° are closely colinear, indicating that $-\Delta H$ is approximately constant in value over this small temperature interval.*

The values of $-\Delta H$ for dissolution of quartz and the two plagioclases are comparable and relatively small, whereas those for the two olivines, while comparable to one another, are very much larger than those of the framework silicates. The data of Watson (1982) and Thornber and Huebner (1982) have been used to obtain the values of $-\Delta H$ for quartz dissolution in basalt and olivine dissolution in a lunar basalt (Table VI), and these too, show a low value for quartz and a very high value for olivine.

Dissolution of minerals in rock melts must involve at least two distinct processes: ions must be extracted from the lattice and enter the melt, and

---

* That the three data points for oligoclase are colinear, despite the fact that the mineral fuses during dissolution at 1300°, implies that there is little difference in the processes of dissolving oligoclase melt and oligoclase crystal in basalt melt; presumably the two phases have very similar structures.

they must then be transported away from the crystal–liquid interface and mixed into the bulk of the melt (e.g. Elwell and Scheel, 1975). Each process has its own activation enthalpy, and its own activated state,† and hence the values of $-\Delta H$ determined from experiments will reflect the most energy-demanding of these processes. It is striking how similar are the values of $-\Delta H$ obtained for the dissolution of quartz and plagioclase to the equivalent parameters for viscous flow of basaltic melt (56 kcal mol^{-1} [Shaw, 1969]) and for tracer diffusion of mono- and divalent cations in silicate melts (30–65 kcal mol^{-1}) (Hofman, 1980; Henderson, 1982). This may indicate that more energy is required to activate the transport of ions from the quartz- and plagioclase-melt interfaces than is needed to activate the extraction of ions from the lattice.

Olivine dissolution has larger values of $-\Delta H$ compared with the values of viscous flow and cation diffusion; these indicate that activation of the reaction(s) that extracts ions from the olivine lattice requires a large energy input. Given the large difference in $-\Delta H$ between the two olivines, it will be interesting to determine the values for more fayalitic olivines, to see if they are less than that for H19.

Rate-controlling step in dissolution. Dissolution

---

† In reality there are probably a series of activated states involved in removing an ion from a crystal (e.g. Elwell and Scheel, 1975, pp. 148–51), each with its own activation energy.

rate depends on whether the reactions that occur at the surface of a dissolving crystal release ions faster or slower than they can be transported away from the crystal. If diffusion of ions in the melt is the dominant rate-controlling step, the dissolution rate ought to be time dependent (Berner, 1980)—specifically, the change in crystal radius should be directly proportional to the *square root* of time, owing to the ever-increasing thickness of 'contaminated' boundary layer of melt. Yet it has been shown (fig. 2 and Table IV) that Δr in fact is proportional to time, not its square root. There are two ways of explaining this relationship, either (*a*) it is the surface reactions which limit the dissolution rate or (*b*) the dissolution rate is limited by steady-state transport conditions involving both diffusion and convection of melt components, specifically diffusion of components through a compositional boundary layer whose thickness remains constant with time and beyond which the melt is mixed by convection (cf. Burton and Slichter, 1958; Kirk-patrick, 1975, 1980): it is the convection that prevents the boundary layer thickening. Situation (*a*) would result in the virtual absence of composition gradients in the melt adjacent to a dissolving crystal, whereas in (*b*) gradients would exist and their thickness would be approximately constant with time.

Fig. 6 illustrates the results of electron microprobe analyses of the glass adjacent to partially dissolved quartz, oligoclase, and olivine crystals. All three exhibit compositional gradients. (Compare the results of Watson (1982) on quartz and feldspar dissolution in basalt, but contrast Thornber and Huebner (1982) who found gradients that indicated *growth* of olivine during quenching.) For example, in fig. 6*a* the melt is enriched in SiO_2 at the crystal–liquid interface and correspondingly depleted in the other oxides [except K_2O which preferentially migrates from the basalt to the contaminated, interfacial melt, cf. Sato (1974) and Watson (1982)]. The 'characteristic thickness', δ, of each gradient, i.e. the distance in which the excess or deficiency of concentration falls or rises to $1/e$ of its original value (Chalmers, 1964, p. 133) is c.10 μm in the quartz example, 100 μm in oligoclase and 75 μm in the olivine* (fig. 6). The actual lengths of the gradients are approximately 100, 400, and 400 μm, respectively. Electron probe traverses have been

obtained for only a small proportion of the total number of runs, however, these reveal no significant differences in either the characteristic thickness or the actual thickness of the concentration gradients with run duration.

It is concluded that in all these experiments transport of ions to and from the crystal–liquid interface is the rate-controlling step; furthermore, the transport takes the form of diffusion through a boundary layer which has a characteristic thickness of the order of 10–100 μm and beyond which some convection occurs. This inference of steady state, *mixed-transport control* of dissolution rate is in accord with investigations of olivine, quartz, and pyroxene dissolution in the system $CaMgSi_2O_6$–Mg_2SiO_4–SiO_2 (Kuo and Kirkpatrick, 1983).

That the convection occurs is surprising and its cause a matter for conjecture. Application of the equation for the thermal Rayleigh number indicates that thermal convection of the bulk melt (e.g. Burton and Slichter, 1958) would not occur unless an impossibly large thermal gradient existed in the experimental charges. Alternatives include convection set up by surface tension variations around the surface of the charge (cf. Tritton, 1977, pp. 204–6), compositional convection caused by flow of relatively light or heavy fluid produced at the crystal–liquid interface (Carruthers, 1976; Huppert and Sparks, 1984), possibly with convective instability of the boundary layer (cf. Turner, 1973, p. 243), and, lastly, random motion of crystals dragging boundary layer melt through the bulk melt. The true nature of the motion must await experiments designed to reveal the three-dimensional form of the boundary layer adjacent to a dissolving crystal.

The enrichment of the interfacial melt in olivine components adjacent to olivine (fig. 6*c*) is trivial by comparison with the large enrichment in SiO_2 adjacent to quartz (fig. 6*a*); despite the large MgO content of the olivine (c.50 wt. %) the basaltic melt is enriched by only 1–1.5 % in MgO at the interface. Coupled with the relatively large values of $-\Delta H$ for olivine dissolution (last section) this suggests that, although transport of components in the melt is the dominant process controlling olivine dissolution rate, the release of ions from the crystal is not a great deal faster. Application of the Roeder and Emslie (1970) olivine–liquid distribution coefficient

$$K_D = \frac{X^{ol}_{FeO} \cdot X^{liq}_{MgO}}{X^{liq}_{FeO} \cdot X^{ol}_{MgO}}$$

to the olivine and the interfacial melt gives values of 0.12–0.20, as opposed to the equilibrium value of 0.30. Clearly the interfacial melt is grossly depleted in MgO for surface equilibrium to pertain. Curiously, despite the olivine in fig. 6*c* containing less FeO than the basalt, there is a slight

---

* There must, for a time, exist a transient condition as the layer of contaminated melt thickens from zero to its steady-state value. During this time dissolution rate will steadily decrease because ions have to diffuse through a growing thickness of melt and because undersaturation at the crystal–liquid interface is steadily reduced. The available data, however, suggest that this transient condition is very short lived, certainly less than half an hour.

FIG. 6. Three examples of the variation in melt (quenched glass) composition adjacent to dissolving crystals. (a) quartz G, run 290. (b) oligoclase, run 289. (c) olivine Ig, run 267. (Note the breaks in vertical scales; in (c) the numbers in brackets refer to potassium.) The approximate major-element composition of the oligoclase is 62 wt. % SiO_2, 22 Al_2O_3, 6 CaO, 7 Na_2O, 0.6 K_2O; that of olivine Ig is 40.5 SiO_2, 50 MgO, 8 FeO.

enrichment in FeO of melt at the interface. This is not understood.

Conclusions

The measured rates of dissolution of olivine, plagioclase, and quartz in basaltic magma differ substantially, raising the possibility that the melt fraction of a magma dissolving megacrysts (whether cognate or truly foreign to the magma) may undergo selective contamination by preferential dissolution of one mineral over another. The results suggest that the melt fraction would enrich in felsic components over mafic ones, assuming all the crystals were of the same size.

The olivine dissolution rates decrease rapidly with falling temperature; close to the liquidus temperature of the basalt olivine dissolves at only 9–14 μm/h. Thus a large olivine Ig phenocryst of 5 mm diameter would require 12 days to dissolve at 1210°. Depending on the rate of ascent and the quantity of olivine phenocrysts in suspension, a basalt moving upwards through the crust could well become both absolutely superheated and increasingly superheated, as the liquidus temperature fell, and yet erupt at the surface or enter a subvolcanic environment with phenocrysts. Perhaps this is why olivine phenocrysts in basalts and olivine primocrysts in some cumulates often have somewhat rounded outlines.

Plagioclase dissolution rates at small degrees of undersaturation seem rapid by comparison with magmatic crystal growth rates at small degrees of supersaturation. For example, the dissolution rate of plagioclase within a few degrees of the plagioclase liquidus temperature of the basalt (1187 °C) is $c.60$ μm/h (extrapolation of data in Table V), whereas Kirkpatrick (1977) estimated the half growth rate of plagioclase in two Hawaiian lava lakes to be approximately three orders of magnitude slower (up to 4×10^{-2} μm/h) at probable small degrees of supercooling. This means that a 10 mm crystal of plagioclase that grew in a lava lake in $c.14$ years, would dissolve in a few days. Thus, even very modest degrees of superheat result in rapid contamination of the melt. This point is reinforced by data of Sato *et al.* (1981) who have measured the growth rates of plagioclase in an aluminous basalt. Extrapolation of their data to a few degrees of supercooling gives a growth rate of 0.35 μm/h, approximately 170 times slower than dissolution at very small superheating. Even at a superheating of 80 °C the dissolution rate is 3–5 times faster than the growth rate of 35 μm Hr measured by Sato *et al.* at 80 °C supercooling.

By contrast, Donaldson (1975) computed growth rates for magnesian olivine in an oceanic tholeiite of 7–20 μm/h. These crystals grew at an unknown value of supercooling but in view of their hopper shapes it was probably several tens of degrees centigrade. Thus olivine growth and dissolution rates seem to be rather similar in magnitude.

Magma does not have to be absolutely superheated in order to dissolve a mineral, only undersaturated with respect to the mineral concerned. Thus, a tholeiitic basalt that acquires a 10 mm diameter crystal of oligoclase at 1150° would dissolve it in $c.35$ days, geologically a trivial amount of time. (See the descriptions of the composite basalt–rhyolite lava/dome at Gardiner River, Wyoming by Wilcox (1944) and of contaminated lavas in the San Juan Mountains of Colorado (Larsen and Irving, 1938) and in the Lassen Volcanic National Park, California (Finch and Anderson, 1930) for classic instances of this situation.)

The most important finding of the study is that, even in the small sample volumes used, dissolution rate is not time dependent. Thermal convection and compositional convection are both very likely to occur in bodies of basaltic magma (Sparks *et al.*, 1984) and so here too there should be no slowing down of dissolution due to an ever-thickening layer of contaminated melt about a dissolving crystal. Depending on the vigour of such convection, the dissolution rates could be faster than those determined in the present study. It will be interesting to examine what happens in more viscous rock melts, in which convection is likely to be much slower. Preliminary results obtained by the author on a melt of 58% SiO_2 suggest that convection may not occur in intermediate composition melts in the beads of melt used in this experimental technique.

A final petrological implication concerns the rate of contamination of the melt fraction of a magma (i.e. weight of dissolved material entering melt per unit time). Whether the dissolution is determined by pure diffusion control or by mixed-transport control, the rate of contamination must decrease with time (assuming that the number of dissolving crystals remains constant). [For example, a plagioclase of 1 mm radius dissolving at 100 μm/h releases 29 mg/h of matter, whereas a crystal of half that radius dissolving at the same rate releases 6.6 mg/h]. However, the rate of decrease in contamination rate will be smaller for the mixed transport situation and, furthermore, the dissolved material will be more rapidly distributed throughout the melt.

the Nuffield Foundation for a Science Research Fellowship, 1983-4, during which this work was done.

REFERENCES

Berner, R. A. (1980) Kinetics of Weathering and Diagenesis. In *Kinetics of Geochemical Processes* (A. C. Lasaga and R. J. Kirkpatrick, eds.), 111–34. Mineral. Soc. Am.

Bond, W. L. (1951) *Rev. Sci. Instrum.* **22**, 344–5.

Bowen, N. L. (1913) *Am. J. Sci.* **35**, 577–99.

——and Schairer, J. F. (1935) *Am. J. Sci.* **26**, 151–217.

Burton, J. A., and Slichter, W. P. (1958) The distribution of solute elements: steady-state growth. In *Transistor Technology*, 1 (H. E. Bridgers, ed.), 71–106. Van Nostrand, New York.

Carruthers, J. A. (1976) *J. Crystal Growth*, **32**, 13–26.

Chalmers, B. (1964) *Principles of Solidification.* 319 pp. Wiley and Sons, New York.

Donaldson, C. H. (1975) *Lithos*, **8**, 163–74.

——(1979a) *Contrib. Mineral. Petrol.* **69**, 21–32.

——(1979b) *Mineral. Mag.* **43**, 115–19.

——Williams, R. J., and Lofgren, G. E. (1975) *Am. Mineral.* **60**, 324–6.

Dowty, E. (1980) Crystal Growth and Nucleation Theory and the Numerical Simulation of Igneous Crystallization. In *Physics of Magmatic Processes* (R. B. Hargraves, ed.), 419–85. Princeton Univ. Press.

Elwell, D., and Scheel, H. J. (1975) *Crystal Growth from High-Temperature Solutions.* Academic Press.

Finch, R. H., and Anderson, C. A. (1930) *Univ. Calif. Dept. Geol. Sci. Bull.* **19**, 245–73.

Harrison, T. M., and Watson, E. B. (1983) *Contrib. Mineral. Petrol.* **84**, 66–72.

Henderson, P. (1982) *Inorganic Geochemistry.* 353 pp. Pergamon Press, Oxford.

Hofman, A. W. (1980) Diffusion in natural silicate melt: a critical review. In *Physics of Magmatic Processes* (R. B. Hargraves, ed.), 385–417. Princeton Univ. Press.

Huppert, H. E., and Sparks, R. S. J. (1984) *Ann. Rev. Earth Planet. Sci.* **12**, 11–37.

Kirkpatrick, R. J. (1975) *Am. Mineral.* **60**, 798–814.

——(1977) *Bull. Geol. Soc. Am.* **88**, 78–84.

——(1980) Kinetics of Crystallization of Igneous Rocks. In *Kinetics of Geochemical Processes* (A. C. Lasaga and R. J. Kirkpatrick, eds.), 321–95. Mineral. Soc. Am.

Kuo, L-C., and Kirkpatrick, R. J. (1983) *EOS (Trans. Am. Geophys. Union)*, **64**, 349.

Kutolin, V. A., and Agafanov, L. V. (1978) *Geol. Geofiz. (Acad. Nauk USSR, Novosibirsk)*, **5**, 3–13.

Lacroix, A. (1893) *Les Enclaves des Roches Volcaniques.* Masson, Paris.

Larsen, E. S., and Irving, J. (1938) *Am. Mineral.* **23**, 227–57.

Lofgren, G. E. (1983) *J. Petrol.* **24**, 229–55.

Moorbath, S., Thompson, R. N., and Oxburgh, E. R. (1984) *Phil. Trans. R. Soc.* **A310**, 437–780.

Roeder, P. L., and Emslie, R. F. (1970) *Contrib. Mineral. Petrol.* **29**, 275–89.

Sato, H. (1974) Ibid. **50**, 49–64.

Sato, K., Kahima, K., and Sunagawa, I. (1981) *J. Jap. Assoc. Petrols. Econ. Geols.* **76**, 294–307.

Sato, M. (1978) *Geophys. Res. Letts.* **5**, 447–9.

Scarfe, C. M., Takahashi, E., and Yoder, H. S. (1980) *Carnegie Inst. Wash. Yearb.* **79**, 290–6.

Shaw, H. R. (1969) *J. Petrol.* **10**, 510–35.

——(1972) *Am. J. Sci.* **272**, 870–93.

Sparks, R. S. J., Huppert, H. E., and Turner, J. S. (1984) *Phil. Trans. R. Soc.* **A310**, 511–34.

Thornber, C. R., and Huebner, J. S. (1982). *EOS (Trans. Am. Geophys. Union)*, **63**, 452–3.

Tritton, D. J. (1977) *Physical Fluid Dynamics.* 362 pp. Van Nostrand, New York.

Turner, J. S. (1973) *Buoyancy Effects in Fluids.* 367 pp. Cambridge Univ. Press.

Watson, E. B. (1982) *Contrib. Mineral. Petrol.* **80**, 73–87.

Wilcox, R. E. (1944) *Bull. Geol. Soc. Amer.* **55**, 1047–80.